Temperature Based Generalized Wavelet-Neural Network Models to Estimate Evapotranspiration in India

Article *in* Information Processing in Agriculture · October 2017

DOI: 10.1016/j.inpa.2017.09.004

1 author:

Sirisha Adamala
ICAR-CIARI

Available at www.sciencedirect.com

INFORMATION PROCESSING IN AGRICULTURE 5 (2018) 149–155

journal homepage: www.elsevier.com/locate/inpa

Temperature based generalized wavelet-neural network models to estimate evapotranspiration in India

Sirisha Adamala *

Applied Engineering Department, Vignan's Foundation for Science, Technology and Research University (VFSTRU), Vadlamdi 522213, India

A R T I C L E I N F O

Article history:
Received 30 December 2016
Received in revised form
22 September 2017
Accepted 28 September 2017
Available online 6 October 2017

Keywords:
Neural networks
Discrete wavelet
Evapotranspiration
Agro-ecological regions

A B S T R A C T

In this paper, generalized wavelet-neural network (WNN) based models were developed for estimating reference evapotranspiration (ET_o) corresponding to Hargreaves (HG) method for different agro-ecological regions (AERs): semi-arid, arid, sub-humid, and humid in India. The input and target to the WNN models are climate data (minimum and maximum air temperature) and ET_o (estimated from FAO-56 Penman Monteith method), respectively. The developed WNN models were compared with the various generalized conventional models such as artificial neural networks (ANN), linear regression (LR), wavelet regression (WR), and HG method to test the best performed model. The performance indices used for the comparison include root mean squared error (RMSE), Nash-Sutcliffe efficiency (NSE), the ratio of average output to the average target ET_o values (R_{ratio}), and relative percentage (RP). The WNN and ANN models were performed better as compared to LR, WR and HG methods. Further, the best performed WNN and ANN models were tested on locations, which were not included in training to test their generalizing capability. It is concluded that the WNN and ANN models were shown good generalizing capability for the tested locations as compared to HG method.

1. Introduction

Accurate estimation of reference evapotranspiration (ET_o) is needed for irrigation scheduling, water resources management, crop yield assessment and hydrological modeling as it is one of the significant components of the hydrologic cycle. To overcome the limitations of existing ET_o methods (direct and indirect), researchers are widely developing the artificial neural network (ANN) based in ET_o models [2–4]. These ANNs have the capability to model the complex non-linear relationship between the air temperature, solar radiation and ET_o. The climate data that needed for accurate estimation of ET_o might cope with non-stationarity. A wavelet transformation (WT) serves as an effective tool for accurately modeling ET_o using various non-stationary hydro-climatic variables by locating the irregular spatial and temporal distributed multi-scale features of data [13]. A number of studies were reported in the literature over the years, on the application of wavelet neural networks (WNNs; combination of ANNs and WT) for modeling different hydro-climatic variables, especially ET_o [1,5,6,9–11,14,15].

The WNN model developed for trained location might be useful only in the developed location unless the external gen-

* Address: Research Field: Soft Computing Applications in Water Resources, India.
E-mail address: sirisha.cae@gmail.com
Peer review under responsibility of China Agricultural University.
https://doi.org/10.1016/j.inpa.2017.09.004
2214-3173

eralizing capability is evaluated, which is not done in most of the studies. If these WNN models are only accurate for the training locations, their real applicability is limited to new locations data, which were not trained. Hence, there is a need to develop generalized WNN (WNN) models which are not only applicable for model training locations but also for outside the training locations. This can be achieved by considering the pooled data of various locations, which have the properties of both spatial and altitudinal variations during training [2–4]. Further, in a developing country like India with higher spatial variation in climate, the required climatic data for ET_o estimation may be extremely hard to obtain at all locations due to the difficulty in observation. The most readily available data for India may be the maximum air temperature (T_{max}) and minimum air temperature (T_{min}). This shows the need of developing WNN models with limited input data i.e. corresponding to Hargreaves (HG) method. Therefore, this study aims: (i) to develop the generalized WNN models corresponding to HG method for four agro-ecological regions (AERs: semi-arid, arid, sub-humid, and humid) of India, (ii) to test the generalizing capability of WNN models with the model development and model testing locations, and (iii) to compare the developed WNN models with the generalized ANN (ANN), generalized linear regression (LR), generalized wavelet regression (WR), and conventional HG method.

2. Study area and climate data

The study area consists a total of 25 different meteorological locations in India (Fig. 1). The data sample consists of daily climate data of T_{min}, T_{max}, and extra terrestrial radiation (R_a). Due to the unavailability of measured lysimeter ET_o data for the selected study locations, it was estimated by the FAO-56 PM method [16]. The classification of climates (AERs) for dif-

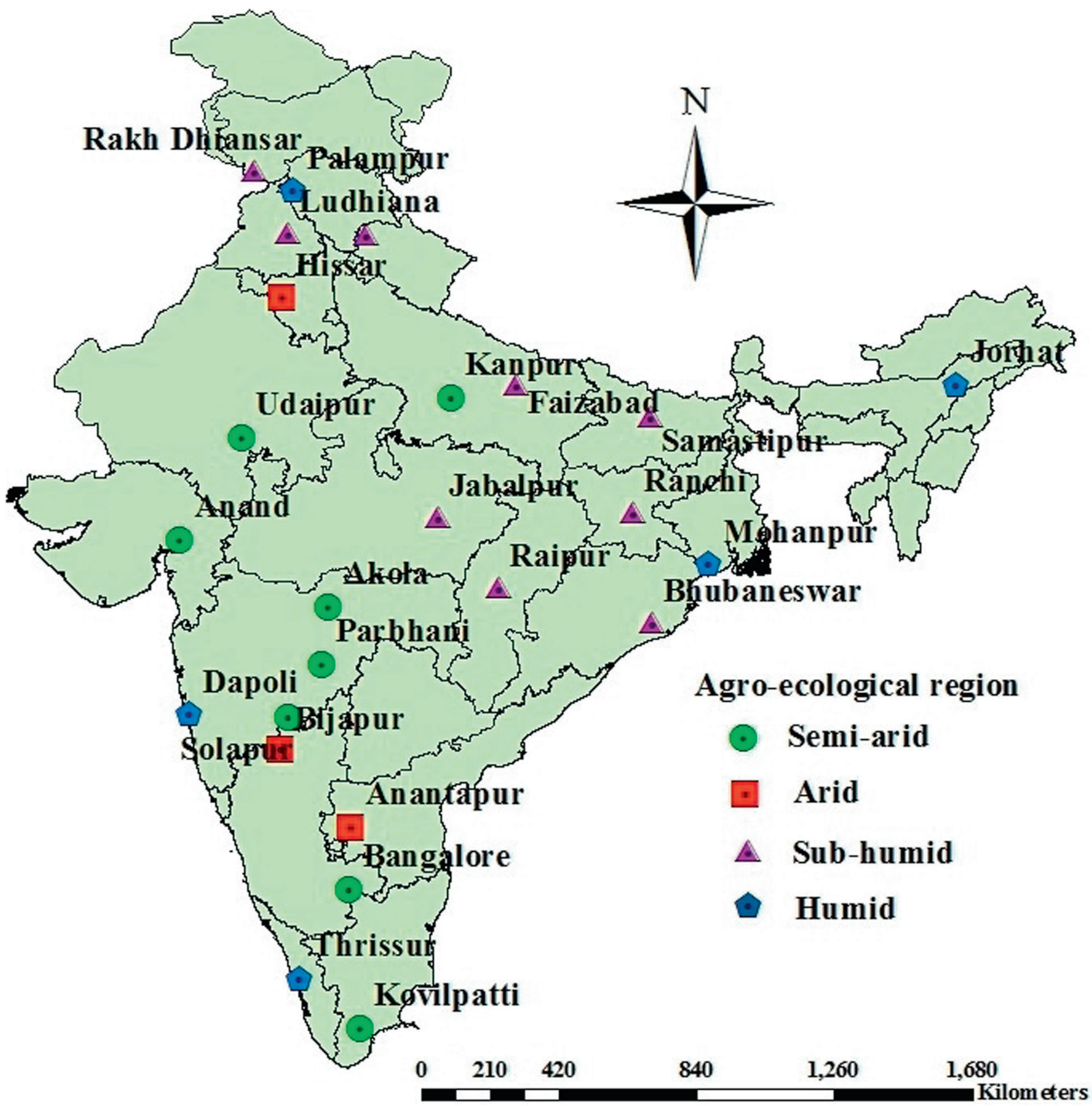

Fig. 1 – Study area (25 climatic stations and four agro-ecological regions).

Table 1 – Characteristics and summary of study locations.

	Location	Lat. (°N)	Lon. (°E)	Alt. (m)	Role[a]	Period
Semi-arid	Parbhani	19°08′	76°50′	423	Tr, V, Ts	2001–05
	Solapur	17°41′	75°56′	25	Tr, V, Ts	2001–05
	Bangalore	12°58′	77°35′	930	Tr, V, Ts	2001–05
	Kovilpatti	9°10′	77°52′	90	Tr, V, Ts	2001–05
	Udaipur	25°21′	74°38′	433	Tr, V, Ts	2001–05
	Kanpur	26°26′	80°22′	126	Ts	2004–05
	Anand	22°33′	72°58′	45	Ts	2002–05
	Akola	20°42′	77°02′	482	Ts	2001–03
Arid	Anantapur	14°41′	77°37′	350	Tr, V, Ts	2001–05
	Hissar	29°10′	75°44′	215	Tr, V, Ts	2001–05
	Bijapur	16°49′	75°43′	594	Ts	2001–04
Sub-humid	Raipur	21°14′	81°39′	298	Tr, V, Ts	2001–05
	Faizabad	26°47′	82°08′	133	Tr, V, Ts	2001–05
	Ludhiana	30°56′	75°52′	247	Tr, V, Ts	2001–05
	Ranichauri	30°52′	78°02′	1600	Tr, V, Ts	2001–05
	Jabalpur	23°09′	79°58′	393	Ts	2002–05
	Samastipur	25°53′	85°48′	52	Ts	2004–05
	Bhubaneshwar	20°15′	85°50′	25	Ts	2002–05
	Ranchi	23°17′	85°19′	625	Ts	2005
	Rakh Dhiansar	32°39′	74°58′	332	Ts	2005
Humid	Palampur	32°06′	76°03′	1291	Tr, V, Ts	2001–05
	Jorhat	26°47′	94°12′	86	Tr, V, Ts	2001–05
	Mohanpur	21°52′	87°26′	10	Tr, V, Ts	2001–05
	Dapoli	17°46′	73°12′	250	Tr, V, Ts	2001–05
	Thrissur	10°31′	76°13′	26	Ts	2001–04

a Tr: Train; V: Validation; and Ts: Test.

ferent locations in the study area is based on 'moisture index' [17].

$$\text{Moisture index, } I_m\ (\%) = 100 * \left[\frac{P}{PET} - 1\right] \tag{1}$$

where P = annual precipitation (mm) and PET = potential evapotranspiration (mm).

Table 1 presents information related to latitude, longitude, altitude, and observation periods for the chosen locations.

3. Description of models and evaluation

3.1. *Hargreaves ET_o estimation method*

The temperature based Hargreaves method [12] that demands fewer climate data for the estimation of ET_o, is described as below:

$$ET_o = 0.0023 R_a \sqrt{TD}(T_{avg} + 17.8) \tag{2}$$

where ET_o = reference evapotranspiration (mm day^{-1}); T_{avg} = average daily air temperature at 2 m height (°C); T_{min} = minimum air temperature (°C); T_{max} = maximum air temperature (°C); TD = difference between T_{max} and T_{min} (°C); R_a = extraterrestrial solar radiation (function of latitude and day of the year) (MJ m^{-2} day^{-1}).

3.2. *Artificial Neural Network (ANN)*

ANN is a massively parallel distributed processor that has a natural propensity for storing experiential knowledge and making it available for use. The ANN employed in this study consists of an input (*i*), hidden (*j*), and an output (*k*) layers with the interconnection weights w_{ij} and w_{jk} between layers of neurons. These can be represented as:

$$y_j = \sum_{i=1}^{n} w_{ij} x_i \tag{3}$$

$$z_k = \phi\left[\sum_{j=1}^{m} w_{jk} y_j\right] \tag{4}$$

where x_i = input vector; y_j = output vector resulted from input to hidden layer; z_k = net output vector; w_{ij} and w_{jk} = set of adaptive parameters (weights) from input to hidden layer and hidden to output layers, respectively; n = number of elements in the input vector; m = number of hidden layers and ϕ = activation function.

The input layer for both the ANN and WNN models consists of three nodes: T_{min}, T_{max}, and R_a and the output layer consists of one node i.e. ET_o (calculated by the FAO-56 PM method). One hidden layer with a different number of hidden neurons was adopted in this study for the design of networks because it can approximate any complex relationship [2,3]. The number of neurons or nodes in the hidden layer and model parameters was generally determined through trial and error. The hidden layer neurons were varied from 1 to 15 in both the developed models. The model parameters that were fixed after a number of trials include 1000 epochs, learning rate of 0.5, and a momentum term as 0.95. Sigmoidal and linear activation functions were employed in the hidden layer and output layer neurons, respectively. For developing both the ANN and WNN, based daily ET_o models, the code was written using Matlab 7.0 programming language (The Mathworks, Inc., Natick, Mass.).

3.3. *Wavelet Transform (WT)*

During the past few decades, the WT appears to be a more effective tool than the Fourier transform (FT) that do not provide an accurate time-frequency analysis for non-stationary signals [7]. The WT analyzes the distorted time-series into different time-frequency scales by detecting the disturbances present in the data. The WT uses two basic functions, i.e. the wavelet (φ) and scaling (Φ) to perform simultaneously the multi-resolution analysis decomposition and reconstruction of the measured time-series data. The high-frequency components (details) are generated by φ whereas Φ generates the low-frequency components (approximations) of the distorted time-series. Discrete wavelet transform (DWT) which is a feature extraction technique translates each time-series from the time domain to the time/frequency domain without losing any information about the instant when the change occurred [8].

$$DWT_{\Psi}x(m,n) = \sum_{k} x_k \Psi^*_{m,n}(k) \quad (5)$$

$$\Psi^*_{m,n}(k) = \frac{1}{\sqrt{a_0^m}} \Psi^*\left(\frac{k - nb_0a_0^m}{a_0^m}\right) \quad (6)$$

where Ψ = mother wavelet function; * = a complex conjugate; a_0^m = scaling factor; $nb_0a_0^m$ = shifting factor; m and n = scaling and sampling numbers, respectively.

Basically, the reconstruction is the reverse process of decomposition. The approximation and detail coefficients at every level are upsampled, passed through the low pass and high pass synthesis filters and then added. This process is continued through the same number of levels as in the decomposition process to obtain the original signal.

3.4. *Development of WNN models*

For developing different WNN models for daily ET_o estimation, the code was written using Matlab programming language. As a priori step in WNN modeling, the data was normalized with a Matlab built-in function called 'mapstd' which maps the data such that it's mean and standard deviations were normalized to 0 and 1, respectively. Further, simulated ET_o with the WNNs were converted back into the original unit by denormalization (using 'mapstd reverse' function) procedure. The input time series (T_{min}, T_{max}, and R_a) was decomposed into different sub-time series components using 'daubechies (db10)' wavelet function (DWT). The pooled climate data for the four AERs is decomposed into ten detailed (D1–D10) and one approximated (A10) components using DWT algorithm [8]. The correlation coefficients of the decomposed climate data with the FAO-56 PM ET_o are shown in Table 2. These decomposition level modes are represented as 2-day (D1), 4-day (D2), 8-day (D3), 16-day (D4), 32-day (D5), 64-day (D6), 128-day (D7), 256-day (D8), 512-day (D9), and 1024-day (D10). Among D1-D10 modes, D8 mode has the highest correlation and D1 and D2 have lowest correlations for all locations with the ET_o. Even, the correlation of D8 level was better than the Approximated mode (A10). Therefore, the annual scale has the greater periodical influence on ET_o estimation for this study area. The correlation coefficient values less than ±0.1 are recognized as ineffective components [15]. Then, these ineffective components can be extracted from the raw data. As results, the reconstructed series is constituted by the added series. The reconstructed data is used for wavelet based models. The ineffective components (shown as 'bold' in Table 2) are eliminated from the raw data and reconstructed series was constituted with the selected components (seen as unbold characters in Table 2) to constitute effective inputs. These effective inputs were used as an input in ANN model to develop the WNN models. Further, these models were compared with the LR, WR, and ANN models. The input to LR and ANN models includes the original climatic time-series data, whereas DWT decomposed effective sub-times series data was used as an input to WR models. The WR model is a conjunction of DWT and LR models.

For the development of WNN models for four AERs, locations having daily data for the period 2001–05 (1826 patterns) were chosen. The locations with 'Tr, V, Ts' role (Table 1) was used to develop WNN models. For these locations, 70% and 30% of data for the period of 2001–04 (1461 patterns) were used for training and validation, respectively. The data for the year 2005 were used for model testing. The data were pooled from (Parbhani, Solapur, Bangalore, Kovilpatti, and Udaipur), (Anantapur and Hissar), (Raipur, Faizabad,

Table 2 – Correlation coefficients of reconstructed climate data with ET_o for four AERs.

AER	Variable	Approximation	Details									
		A10	D1	D2	D3	D4	D5	D6	D7	D8	D9	D10
Semi-arid	T_{max}	0.40	**0.08**	0.11	0.12	0.12	0.10	0.13	0.29	0.55	0.14	0.15
	T_{min}	0.40	**0.03**	**0.03**	**0.02**	**0.03**	**0.01**	**0.06**	0.17	0.42	**0.07**	0.11
Arid	T_{max}	0.34	**0.04**	0.11	0.12	0.11	0.11	0.13	0.19	0.66	**0.03**	**−0.03**
	T_{min}	0.36	**0.02**	**0.06**	**0.07**	**0.05**	**0.06**	**0.09**	0.27	0.61	**0.08**	**−0.03**
Sub-humid	T_{max}	**0.03**	**0.07**	0.11	0.11	0.13	0.10	**0.09**	0.31	0.78	0.12	**0.02**
	T_{min}	**0.00**	**0.03**	**0.05**	**0.05**	**0.06**	**0.05**	**0.06**	0.23	0.69	0.11	**0.03**
Humid	T_{max}	0.16	**−0.02**	**0.09**	0.17	0.18	0.14	0.13	0.37	0.58	0.18	**0.05**
	T_{min}	0.12	**0.00**	**0.03**	**0.05**	**0.06**	**0.02**	**0.01**	0.30	0.51	0.14	**0.01**

Table 3 – Performance statistics of generalized models under four AERs during testing.

Model	Semi-arid				Arid				Sub-humid				Humid			
	RMSE	NSE	R_{ratio}	RP[a]	RMSE	NSE	R_{ratio}	RP[a]	RMSE	NSE	R_{ratio}	RP[a]	RMSE	NSE	R_{ratio}	RP[a]
HG	1.062	54.68	1.139	–	1.247	65.98	0.919	–	1.058	67.02	1.172	–	0.959	44.75	1.199	–
LR	1.052	57.81	1.015	0.94	1.257	65.43	1.015	−0.80	1.075	65.96	1.027	−1.61	0.892	52.28	1.022	6.99
WR	1.040	58.76	1.014	2.07	1.236	66.58	1.014	0.88	1.063	66.71	1.029	−0.47	0.877	53.83	1.020	8.55
ANN	0.682	82.26	1.010	35.78	1.023	77.09	0.996	17.96	0.671	87.06	0.992	36.58	0.663	73.62	0.993	30.87
WNN	0.658	83.47	1.006	38.04	0.925	81.26	0.996	25.82	0.659	87.40	0.998	37.71	0.628	76.32	0.993	34.52

Note: RMSE = mm day^{-1}; R_{ratio} = dimensionless; RP = %; and NSE = %.
* RP is the relative percentage change in RMSE of LR, WR, ANN, and WNN models over HG method.

Table 4 – Average ET_o values of different models under four AERs during testing.

Region	Target ET_o	WNN	ANN	WR	LR	HG
Semi-arid	4.193	4.217	4.235	4.251	4.255	5.140
Arid	4.997	4.977	4.978	5.064	5.074	5.093
Humid	3.892	3.856	3.851	3.473	3.489	3.770
Sub-humid	3.269	3.207	3.322	3.958	3.970	4.555

Ludhiana, and Ranichauri), and (Palampur, Jorhat, Mohanpur, and Dapoli) locations to develop WNN models for semi-arid, arid, sub-humid, and humid regions, respectively. To test the generalizing capability of the WNN models, the data from remaining locations that were not used during model development which consist different observation periods were used. The locations with only 'Ts' role (Table 1) was used to test the generalizing capability of the developed models (model testing locations). It is worth to mention that due to lack of availability of climate data for the humid region, only one station (Thrissur) data is used to test the generalizing capability of developed models under this region.

3.5. *Performance evaluation*

The root mean squared error (RMSE), Nash-Sutcliffe efficiency (NSE), the ratio of average output to the average target ET_o values (R_{ratio}), and relative percentage (RP) are used to evaluate the performance of various models. The expressions for these indices are described below:

$$\mathrm{RMSE} = \sqrt{\frac{1}{n}\sum_{i=1}^{n}(T_i - O_i)^2} \tag{7}$$

$$\mathrm{NSE} = \left[1 - \frac{\sum_{i=1}^{n}(T_i - O_i)^2}{\sum_{i=1}^{n}(T_i - \overline{T})^2}\right] * 100 \tag{8}$$

$$R_{ratio} = \frac{\overline{O}}{\overline{T}} \tag{9}$$

$$\mathrm{RP} = \left(\frac{\mathrm{RMSE}_1 - \mathrm{RMSE}_2}{\mathrm{RMSE}_1}\right) * 100 \tag{10}$$

where T_i and O_i = target and output values, respectively; n = number of data points; $\overline{O}$ and $\overline{T}$ = average of output and target values, respectively, RMSE_1 = RMSE of conventional method; RMSE_2 = RMSE of wavelet models.

4. Simulation results and discussion

This section presents the best achieved results of WNN models corresponding to HG method for four AERs during testing. To find the accuracy of WNN models, these were compared with the LR, WR, and ANN models. Table 3 shows that the performance of LR, WR, ANN, and WNN models in terms of RMSE, NSE, and R_{ratio} under four AERs during testing (2005 year pooled data). Among all developed models, the WNN models are the best models with the lowest RMSE (mm day^{-1}) values of 0.658, 0.925, 0.659, and 0.628 for semi-arid, arid, sub-humid, and humid regions, respectively. Here, it is worth to mention that the R_{ratio} is used only to know whether the models overestimated ($R_{ratio} > 1$) or underestimated ($R_{ratio} < 1$) simulated ET_o values. The developed WNN, ANN, WR, and LR models were also compared with the conventional HG method to find the accuracy of former models over conventional methods. The RP values in Table 3 indicates that the relative percentage change in RMSE of LR, WR, ANN, and WNN models over conventional HG method. The relative performance of ANN and WNN models was about 17–38% better as compared to HG method for semi-arid, arid, sub-humid, and humid regions. But the LR and WR models were performed more are similar (RP = 1–8%) as compared to HG method for semi-arid, arid, sub-humid, and humid regions. The negative RP values in Table 3 indicate that the better performance of conventional HG method as compared to LR and WR models. In some areas, data of the climatic parameters other than air temperature are not available; in such cases practicing engineers should use either WNN or ANN models for accurate estimation of ET_o instead of other methods. Therefore, WNN models will have a greater potential application in modeling ET_o under different AERs of India. Similar best performance of wavelet based models was achieved by [14,15]. Table 4 shows the mean annual (mm day^{-1}) values of target ET_o (estimated with FAO-56 PM equation), WNN,

Table 5 – Performance of generalized models for model development locations.

AER	Location	HG			ANN			WNN		
		RMSE	NSE	R_{ratio}	RMSE	NSE	R_{ratio}	RMSE	NSE	R_{ratio}
Semi-arid	*Parbhani*	1.057	56.44	1.180	0.649	83.59	0.987	0.925	81.26	0.996
	Solapur	1.001	57.34	1.148	0.708	78.66	0.977	0.759	75.47	0.975
	Bangalore	1.018	17.82	1.013	0.664	65.05	0.981	0.691	62.07	0.983
	Kovilpatti	1.785	−34.09	1.118	1.026	54.00	1.039	1.163	43.07	0.924
	Udaipur	1.025	70.00	1.017	0.785	82.41	1.026	1.257	54.92	0.817
Arid	*Anantapur*	1.392	40.29	0.983	1.094	63.15	0.964	1.394	40.11	0.927
	Hissar	1.223	61.15	1.065	0.839	81.73	0.988	1.276	57.75	0.813
Sub-humid	*Raipur*	1.122	59.01	1.036	0.713	82.01	0.976	0.738	82.23	0.964
	Faizabad	1.265	45.86	0.908	0.623	86.87	0.992	0.641	86.08	0.989
	Ludhiana	1.078	71.64	0.938	0.659	89.56	1.008	0.621	90.59	1.032
	Ranchi	1.110	31.99	0.715	0.602	76.48	1.067	0.541	83.80	1.021
Humid	*Palampur*	0.759	71.54	0.964	0.691	77.36	0.996	0.611	81.51	1.010
	Jorhat	1.370	−78.84	0.689	0.706	54.24	0.975	0.613	64.13	0.967
	Mohanpur	1.801	−90.52	0.627	0.647	75.58	0.963	0.667	73.79	0.977
	Dapoli	1.129	−9.915	1.263	0.621	65.72	0.909	0.738	53.01	0.926

WR, LR and Hargreaves methods. It is concluded from the Table 4 that the WR, LR and HG models showed a larger variation in average annual ET_o as compared to FAO-56 PM ET_o.

4.1. *Testing generalizing capability of WNN models*

The generalizing capability of LR, WR, ANN, and WNN models was tested with 'model development' and 'model testing' locations. In order to highlight the necessity of developing different ANN and WNN models, it is necessary to first show the results obtained using conventional ET_o method (HG). Table 5 shows the performance statistics of ANN, WNN and conventional HG models in terms of RMSE, NSE, and R_{ratio} with the model development locations under four AERs. The RMSE values range from 0.759 to 1.801 mm day^{-1} for HG method, whereas the range of RMSE values for ANN and WNN models were 0.602–1.094 mm day^{-1} and 0.541–1.394 mm day^{-1}, respectively. Similarly, the NSE values for HG, ANN and WNN models range from −90.52 to 71.64%, 54.0 to 89.56%, and 40.11 to 90.59%, respectively. Among the HG, ANN and WNN models, the ANN models showed the low RMSE and high NSE values for most of the locations. Next to ANN models, the WNN models showed the superior performance as compared to HG method. Thus, from these results it can be concluded that both the ANN and WNN models were showed their superiority as compared to HG models. These superior results indicated that the performance of WNN and ANN models during testing the generalizing capability with the model development locations was best.

Table 6 illustrates the performance statistics of ANN and WNN models in terms of RMSE, NSE, and R_{ratio} with the model testing locations under four AERs. The performance of best performed models (i.e. ANN and WNN) was compared with the conventional HG method. The RMSE values range from 0.932 to 1.55 mm day^{-1} for HG method, whereas the range of RMSE values for ANN and WNN models were 0.571–1.493 mm day^{-1} and 0.632–1.692 mm day^{-1}, respectively. Similarly, the NSE values for HG, ANN and WNN models range from 26.35 to 69.99%, 42.1 to 85.78%, and 39.53 to 84.16%, respectively. Among the HG, ANN and WNN models, the ANN mod-

Table 6 – Performance statistics of generalized models with the model testing locations.

AER	Location	HG			ANN			WNN		
		RMSE	NSE	R_{ratio}	RMSE	NSE	R_{ratio}	RMSE	NSE	R_{ratio}
Semi-arid	Kanpur	1.058	69.99	1.149	0.855	79.99	1.051	1.212	60.57	0.845
	Anand	1.146	39.24	1.187	0.619	78.26	0.981	0.737	74.84	0.911
	Akola	1.519	62.14	1.004	1.097	80.36	0.968	1.692	53.01	0.815
Arid	Bijapur	1.023	33.77	1.172	0.746	67.68	0.940	0.919	46.48	0.904
Sub-humid	Jabalpur	1.208	51.16	1.209	0.681	85.78	0.990	0.709	83.16	0.984
	Samastipur	0.942	64.45	1.095	0.692	80.25	0.993	0.675	81.67	0.998
	Bhubaneshwar	1.007	62.49	1.082	0.871	72.58	0.982	0.804	76.09	0.982
	Ranichauri	1.277	30.52	1.301	0.571	75.45	0.981	0.632	75.96	0.985
	Rakh Dhiansar	1.550	26.35	1.414	0.653	82.76	1.024	0.639	84.16	1.029
Humid	Thrissur	0.932	46.31	1.036	1.493	42.10	0.961	1.5292	39.53	0.930

els showed low RMSE and high NSE values for most of the testing locations. Next to ANN models, the WNN models showed the superior performance as compared to HG method. Thus, the generalizing capability of ANN and WNN models was better as compared to HG method for all locations. The efforts in developing the complex ANN and WNN models were justified with their superior performance in estimating accurate ET_o. The above results are quite encouraging and suggest the usefulness of WNN modeling techniques as an alternative to ANN, LR, WR, and conventional estimation approaches for accurate estimation of ET_o.

5. Conclusions

The performance of the generalized wavelet based neural network (WNN) models with limited climate data (maximum and minimum air temperature) for the estimation of ET_o has been evaluated in this study. The WNN models were developed by considering pooled daily climate data for a period of five years for four AERs in India. The performance of developed WNN models was compared with the ANN, LR, WR, and conventional HG method using various performance indicators. Performance results of the WNN models were very satisfactory as these models gave lowest RMSE and highest NSE values for most of the locations as compared to the ANN, WR, and LR models. Further, the WNN models were applied to models development and model testing locations to test the generalizing capability. During testing generalizing capability with the 15 model development locations and 10 model testing locations, the ANN and WNN models performed better for most of the locations. The WR and LR models showed least performance for almost all locations during testing generalizing capability. Further, all WNN, ANN, WR, and LR models performed much better than their corresponding conventional methods. Therefore from the above results, it is concluded that both the WNN and ANN models can successfully be employed in modeling ET_o for different locations in India. However, it should be noted that this study used data only from different climates in India and thus the results might be different for other climates around the world. Further, these models need to be tested on more climatic locations of India and they can be developed with monthly climatic data. Furthermore, the uncertainty associated in ET_o estimation of different WNN models may be addressed in future studies using bootstrap technique.

REFERENCES

[1] Abghari H, Ahmadi H, Besharat S, Rezaverdinejad V. Prediction of daily pan evaporation using wavelet neural networks. Water Resour Manage 2012;26:3639–52.

[2] Adamala S, Raghuwanshi NS, Mishra A, Tiwari MK. Evapotranspiration modeling using second-order neural networks. J Hydrol Eng 2014;19(6):1131–40.

[3] Adamala S, Raghuwanshi NS, Mishra A, Tiwari MK. Development of generalized higher-order synaptic neural-based ETo models for different agroecological regions in India. J Irrig Drain Eng 2014;140(12).

[4] Adamala S, Raghuwanshi NS, Mishra A. Generalized quadratic synaptic neural networks for ET_o modeling. Environ Process 2015;2(2):309–29.

[5] Cannas B, Fanni A, See L, Sias G. Data processing for river flow forecasting using neural networks: wavelet transforms and data partitioning. Phys Chem Earth 2006;31:1164–71.

[6] Cobaner M. Reference evapotranspiration based on Class A Pan evaporation via wavelet regression technique. Irrig Sci 2013;13:119–34.

[7] Coulibaly P, Burn DH. Wavelet analysis of variability in annual Canadian streamflows. Water Resour Res 2004;40(3):1–14.

[8] Daubechies I. Ten lectures on wavelets. Soc Ind Appl Math 1992:357.

[9] Drago AF, Boxall SR. Use of the wavelet transform on hydrometeorological data. Phys Chem Earth 2002;27:1387–99.

[10] Evrendilek F. Assessing neural networks with wavelet denoising and regression models in predicting diel dynamics of eddy covariance-measured latent and sensible heat fluxes, and evapotranspiration. Neural Comput Appl 2014;24:327–37.

[11] Falamarzi Y, Palizdan N, Huang YF, Lee TS. Estimating evapotranspiration from temperature and wind speed data using artificial and wavelet neural networks (WNNs). Agric Water Manage 2014;140:26–36.

[12] Hargreaves GH, Samani ZA. Reference crop evapotranspiration from temperature. Appl Eng Agric 1985;1(2):96–9.

[13] Izadifar Z, Elshorbagy A. Data driven techniques and wavelet analysis for the modeling and analysis of actual evapotranspiration; 2013. https://doi.org/10.5772/52809.

[14] Kisi O. Evapotranspiration modeling using a wavelet regression model. Irrig Sci 2011;29:241–52.

[15] Partal T. Modelling evapotranspiration using discrete wavelet transform and neural networks. Hydrol Process 2009;23:3545–55.

[16] Debnath S, Adamala S, Raghuwanshi NS. Sensitivity analysis of FAO-56 Penman-Monteith method for different agro-ecological regions of India. Environ Process 2015;2(4):689–704. https://doi.org/10.1007/s40710-015-0107-1.

[17] Thornthwaite CW, Mather JR. The water balance. Publ Climatol Lab Climatol Centerton NJ 1955;8(1):104.